TRANSPORT PROBLEMS 2020 Volume 15 Issue 2
PROBLEMY TRANSPORTU DOI: 10.21307/tp-2020-026

Keywords: traffic streams; aerodynamic interaction; pollution dispersion

Valerii SOLODOV
Kharkiv National Automobile and Highway University
Yaroslav Mudrii str. 25, Kharkiv, 61024, Ukraine
Corresponding author. E-mail: solodov.v@gmail.com

PROBLEM OF AERODYNAMIC INTERACTION OF TRAFFIC STREAMS

Summary. This study presents a model of continuous oncoming traffic flows of vehicles along highways. The flow of atmospheric air and impurity particles is modeled numerically based on unsteady Reynolds-Averaged Navier–Stokes equations using the *MTFS*® authoring software. Detailing of the flow patterns allows arbitrary length regions of periodicity, taking into account a crosswind. The examples provided demonstrate some of the results of the aerodynamic interaction of two oncoming columns of vehicles. The model of aerodynamic interaction of vehicles in traffic on a straight section of road in tunnels allows an arbitrary number of vehicles in each sub-region, along with an arbitrary, periodically repeating configuration of vegetation and buildings on the side of the road to be considered.

1. INTRODUCTION

The influence of large trucks on the aerodynamics of cars during overtaking maneuvers on highways has been considered since the 1970s, mainly experimentally. Experimental studies in the 1980s showed the importance of taking into account and reducing lateral gusts of wind on highways to improve traffic safety. Therefore, in [8], it was shown that when a gust of wind occurs on a dry road surface with normalized adhesion, the lateral pull of a small car at a speed of 90 km/h could be up to 2 meters in an interval of about 2 seconds. In this respect, in most studies, a quasi-stationary experiment was conducted on small models [1] in a wind tunnel to study the aerodynamic characteristics of a small car in the immediate vicinity of a large truck. Yaw measurements were included in the experiment to approximately simulate gusts and crosswind effects.

Goetz [2, 3] studied bodies' design of sedans, buses and the effect of their aerodynamics. Howell [4] investigated the aerodynamics of a car in proximity to a truck using small models. The effects of the shape of the car and the lateral distance between the truck and the car were also investigated. The highest lateral force coefficients were obtained for a station wagon. The length of the truck was also varied and showed that a significant contribution to the impact on the car when passing the cabin and rear of the truck can also be represented on a short truck body. Heffley [5] considered aerodynamics of model passenger cars in close proximity to trucks and buses. Brown and Seeman [6] performed a dynamic experiment using models ejected along parallel tracks and a tailwind generator.

Telionis et al. [7] also conducted a dynamic small-scale experiment for a passing truck using towing. The lateral effect on the coefficients of force and yaw moment was insignificant, and depended on the difference in speeds between cars and trucks.

Hucho [9] summarized the achievements in cars aerodynamics, but on the models mainly.

Yamamoto et al. [10] conducted numerous experiments on the effects of a passing bus in static, and the dynamics of wind tunnel tests, as well as a full-scale study on the road itself. From these experiments, a general conclusion was drawn that, for small relative overtaking speeds, static tests

were adequate. In the case of dynamic full-scale tests for the scenario when a bus overtakes a car, it was found that, at higher relative speeds, the coefficients of peak lateral force and yaw moment increased.

Széchényi [11, 13] conducted a thorough analysis of the overtaking process on rail systems with the possibility of yaw. Also, a number of authors, for example [4], [6], [12], showed that peak loads increase with a decrease in lateral displacement between vehicles.

Schrefl et al. [14] presented preliminary results for surface pressure measurements for on-road tests during a highway passing maneuver.

Noger [12, 15], along with a group of authors, conducted a detailed full-scale simulation of overtaking in a wind tunnel. Howell et al. [17] conducted a detailed review of the aerodynamics of overtaking a long road train with a small car.

Based on this review, we can conclude that the aerodynamic interaction of vehicles has been studied mostly experimentally, using a scenario involving a pair of cars as an example, usually quasi-static and of model sizes.

In this respect, it seems appropriate to conduct a dynamic study of the interaction of full-size numerical models involving two or more cars. At the same time, it also seems relevant to study the wake of the car and the degree of gas contamination on the surrounding space.

Construction of new generation highways implies an increase in the average speed of movement as well as improvement of traffic safety measures. In this respect, the study of the aerodynamics of the flow of vehicles, which is formed under the influence of meteorological conditions near highways, Rose of Wind, traffic intensity and the quality of aerospace planning adjacent to the highway, acquires particular relevance.

2. FORMULATING THE PROBLEM OF AERODYNAMIC INTERACTION OF TRANSPORT

Below, we propose a mathematical and numerical model of the aerodynamic interaction of vehicle traffic flows using an example of a selected fragment of a transport highway, which is shown on a horizontal plane in Fig. 1. The fragment contains subareas OA_1B_1O and OA_2B_2O, which move and contain vehicles, and areas $A_2A_3B_2B_3$ and $A_0A_1B_0B_1$, which simulate the spaces of fixed sidelines. On the sidelines, there may be buildings, vegetation, walls of large buildings, the tunnels or crossroads. Furthermore, we consider this fragment to be representative from the point of view of the determining influence of its elements on the state of the atmosphere over the road.

The airflow in the selected fragment of the transport highway is modeled numerically based on the non-stationary Reynolds-Averaged Navier–Stokes equations, with closure by a suitable model of turbulent viscosity

$$div\,\vec{v} = 0 \tag{1}$$

$$\frac{\partial \vec{v}}{\partial t} + \left(\vec{v}\cdot\nabla\right)\vec{v} = -\frac{\nabla p}{\rho} + \eta\frac{\Delta\vec{v}}{\rho} + \vec{F} \tag{2}$$

The impurity c transfer equation has the form:

$$\frac{\partial c}{\partial t} + \left(\vec{v}\cdot\nabla\right)c = \mu\Delta c + S_c \tag{3}$$

where $\vec{v}-$ velocity, $p,\ \rho-$ pressure, density, S_c- the power of the polluting source, $\vec{F}-$ the power of the impulse source, $\mu-$ the coefficient of turbulent diffusion and $\eta-$ the coefficient of turbulent viscosity.

To simulate the turbulent effects of transport, a two-parameter differential turbulence model k - ε with wall functions and compressibility correction was used [18-20]. Its efficiency and cost-effectiveness for impurity transfer modeling problems were discussed in [18]. Transport equations for k and ε parameters of the model can be found, for example, in [18, 19]. Constants and a detailed description of the model can be found in [19], for example.

Vegetation on the sidelines can be represented as a set of sections of a porous medium with varying degrees of porosity. Its influence can be taken into account using the source terms in the right-hand sides of the momentum equations in the form of a generalized form of Darcy's law [20]. Source term has a form

$$\vec{F} = -C_1\vec{v} - C_2\left|\vec{v}\right|\vec{v} \tag{4}$$

Atmospheric environment can be described as a mixture of gases of a constant density [21].

The task is to determine the main gas-dynamic parameters of the atmospheric wake: pressure, velocity components of the medium, as well as impurity parameters on the part of the transport highway in Euler variables in the presence of moving vehicles.

The study was carried out using the software package *MTFS*® [22], in which the basic implicit algorithm is based on splitting using the method of alternate directions and a TVD (Total Variation Diminishing) scheme of the second order of accuracy with correction of compressibility. The organization of calculations uses a variant of the algorithm with splitting the computing process for multiprocessor platforms. The solid walls are assumed to be adiabatic, with no slipping condition set on them. The flow model is considered as a two-speed (air + CO) model of motion of a mixture of non-interacting gases.

During modeling, a grid description of the computational domain with a condensed grid near the walls of vehicles and the roadway is used. In the fixed observer reference system, the grid spaces of sub-regions 1 and 2 with sets of moving vehicles glide relative to each other in the air, which they carry away with them due to aerodynamic and viscous interaction.

The flows in each of the sub-regions OA_1B_1O and OA_2B_2O are described in moving reference frames, and are relative. In these reference systems, the groups' vehicles are stationary, but the air, road surface and possible stationary objects on wayside spaces move at opposite speeds.

Setting the boundary conditions for each sub-region along surfaces O-O, A_1B_1 and A_2B_2 is based on the interaction of regions by recalculating the flux vectors of gas-dynamic quantities from one reference frame to another. Regions of periodicity on both sides of the surfaces can have an arbitrary length and can include an arbitrary number of participants in the movement. At different lengths of sub-regions on both sides of the surface of O–O, the flow vectors are interpolated, taking into account the periodicity of flow patterns.

The implementation of the algorithm for transmitting flows across the O–O boundary depends on the choice of the finite-volume scheme for integrating the Navier–Stokes equations, and is determined by the programmer.

The selection in Fig. 1 of just a two-lane freeway does not reduce the generality of the proposed approach. There may be several lanes; selected areas may contain from one to several vehicles. Sub-regions can have different lengths and widths. The length of the sub-region refers to the length of the periodicity of the repetition of the structure, i.e. if the length of the sub-region is short in the direction of the centerline, the repetition of the structure should be frequent.

There are some restrictions on this problem statement. In particular, the section of the road is considered to be straight, the vehicles inside the sub-regions do not maneuver and they move with the speed of movement of the sub-regions. At the boundaries of the entire region (Fig. 1) along the line of motion, it is assumed to continue periodically, neglecting the influence of possible non-periodic external elements of motion, terrain features, external atmospheric conditions and disturbances. Here, maneuvering means a reduction in distance, overtaking when leaving your lane or stopping. The road section is considered to be straight, but this restriction can be overcome by introducing fragments of the freeway of variable curvature.

The second variant of the continuation could be, for example, the equality to zero of the derivatives of gas-dynamic parameters at boundaries A_1A_2, B_1B_2, A_2A_3, B_2B_3, A_0A_1 and B_0B_1 (Fig. 1). Namely, this variant is the most appropriate for the modeling of single-car movement.

Below, we consider some examples of the first variant for the case of two-lane traffic. Let the first side of the fragment contain n_1 motion elements and let the second side contain n_2 motion elements. We consider the uniform motion of elements with constant speed and no overtaking. In the absolute frame of reference associated with a fixed surface of the road, the first group moves at a speed of v_1 and the second group moves at a speed of v_2 relative to a fixed observer on the side of the road.

The directions along the highway and magnitudes of the velocity of the groups are arbitrary, the distances between the elements in the groups are arbitrary too, as are the dimensions and configuration of the elements, and they are determined by the objectives of the study and the capabilities of computing equipment.

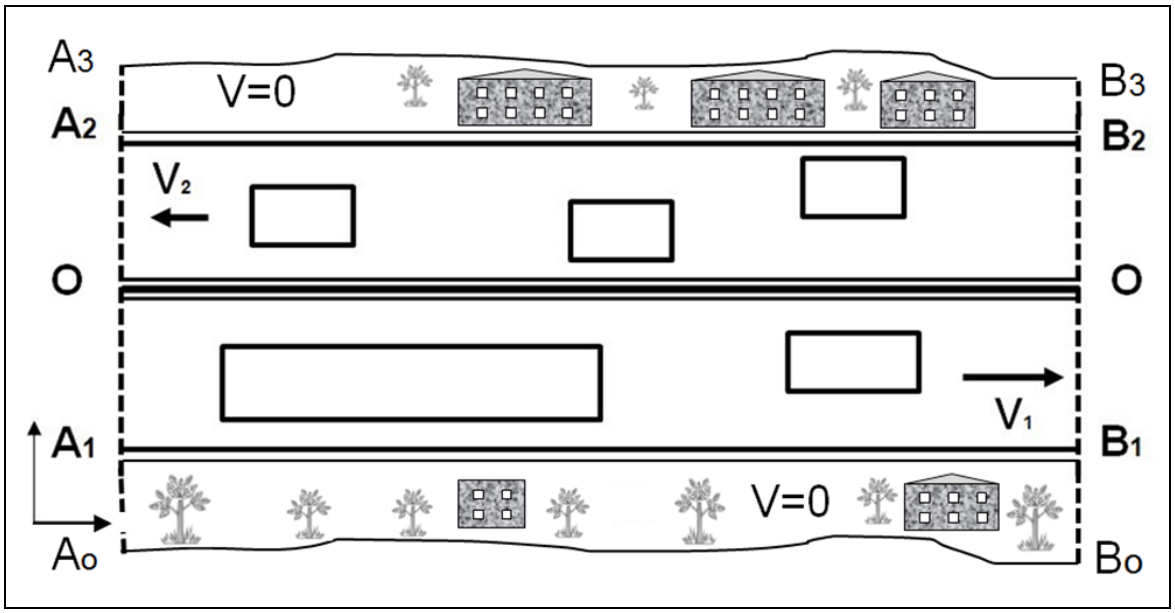

Fig. 1. Illustration of the calculation region

3. DISCUSSION OF THE EXAMPLES

To demonstrate the operability of the proposed formulation, examples of the aerodynamic interaction of bus and passenger cars in oncoming traffic are considered below.

For buses (Fig. 2), the dimensions of the dive area are 60x12x12 m^3; the dimensions of each transport are 10x3x3 m^3. Vehicles are modeled in a simplified manner without wheels, and move at a height of 1 m from the roadway; lateral distances between cars are 3m. Each vehicle is fitted with an exponentially condensed mesh to create a boundary layer model, and a boundary layer is modeled on the road surface. For the calculation, the speed of each sub-region is set, for example, 16 m/s, and a stationary calculation is performed. Next, the unsteady calculation algorithm [22], developed by the author earlier [23], is applied to the aerodynamic interaction of mutually moving grids of the turbine stage.

For accurate modeling of the wake behind the car, its turbulence characteristics, the resulting diffusion of exhaust particles and the grid filling the space of each sub-region should be quite small. In this case, unsteady calculation is forcibly implemented by a small time-step, which places increased demands on the computing system.

The demonstration examples used mid-level grids and the rate of extracting CO from the estimated data [24]. According to [24], the estimated CO emission for a loaded truck may be 3-5E-6 kg/s. In this

example, the exhaust rate of CO 5E-6 kg/s was used. The conditions of modeling were as follows: temperature 300K, atmospheric pressure and CO emission from exhaust pipes occurring at a temperature of 330K and a speed of 0.1 m/s.

In Fig. 2, for the case of oncoming traffic, the isolines of the velocity of the mass fraction of CO in the fixed reference system, the lines of the level of the mass fraction of CO and the surface of the air velocity level with a value of 14 m/s are presented. The graphs also show the distribution of absolute speed in the wake of the bus along the height in three positions: in the center of wake (2), as well as left (3) and right (1).

For a stationary observer, the lower bus in Fig. 2 moves to the right, which is equivalent to the movement of air to the left for a moving observer. Behind the bus, there are air velocity distributions in the stationary frame of reference at the edges and in the center of the bus.

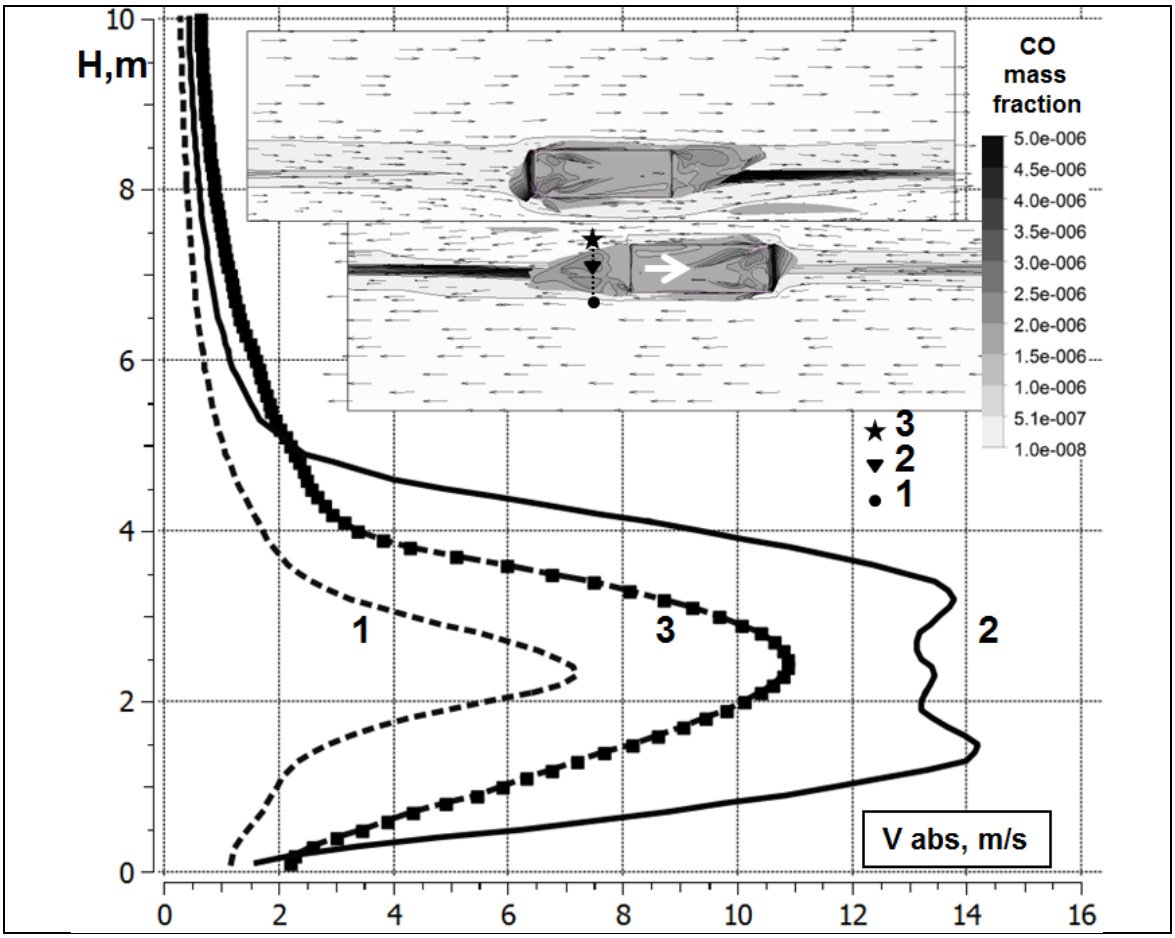

Fig. 2. Flow pattern near the buses and velocity distributions for the absolute observer

The highest speed was recorded in the center of the bus, and the increase in speed between buses due to the narrowing of the channel was also noted; the speed on the outside of the bus is low and drops to zero on the side of the road. As already mentioned, the flow pattern must be periodic; thus, the vehicle runs on the trace ahead of the vehicle in front.

Air velocity vectors are given in moving reference systems associated with automobiles. Unsteady flow in this example is root mean square averaged for flow patterns.

Figs. 3-7 show the results of a more complex scenario of the interaction of traffic streams. The motorcades use models of buses, a truck and a car. The parameters of the bus are taken from the first example, the truck is two times shorter and the car has the dimensions 4x2x1.5m^3.

The following boundary conditions were used to calculate two motorcades: a wind speed of 2m/s, atmospheric pressure, a temperature of 300K, with CO emission from exhaust pipes occurring at a temperature of 330K and a speed of 0.1m/s. The mass flow rate of CO from the exhaust pipe of a passenger car was 1.0E-06 kg/s. The resistance of the windward side stands was set by first loss coefficient C_1=0; second loss coefficient of C_2=0.5 m^{-1}, and from the lee side – C_1=0, C_2=0.1 m^{-1}.

Figure 3a shows a fragment of a traffic stream with a repeating structure of traffic participants: 3 cars (to the right) at a speed of 16 m/s and 2 cars (to the left) at the same speed. On the roadsides, there are fixed stands of the same structure and size. Arrows show the direction of the crosswind. Along the centerline, vertically upward at a height of 0.6 m above the roadway, the OX axis is specified, which is used in the graphs of Fig. 6-7.

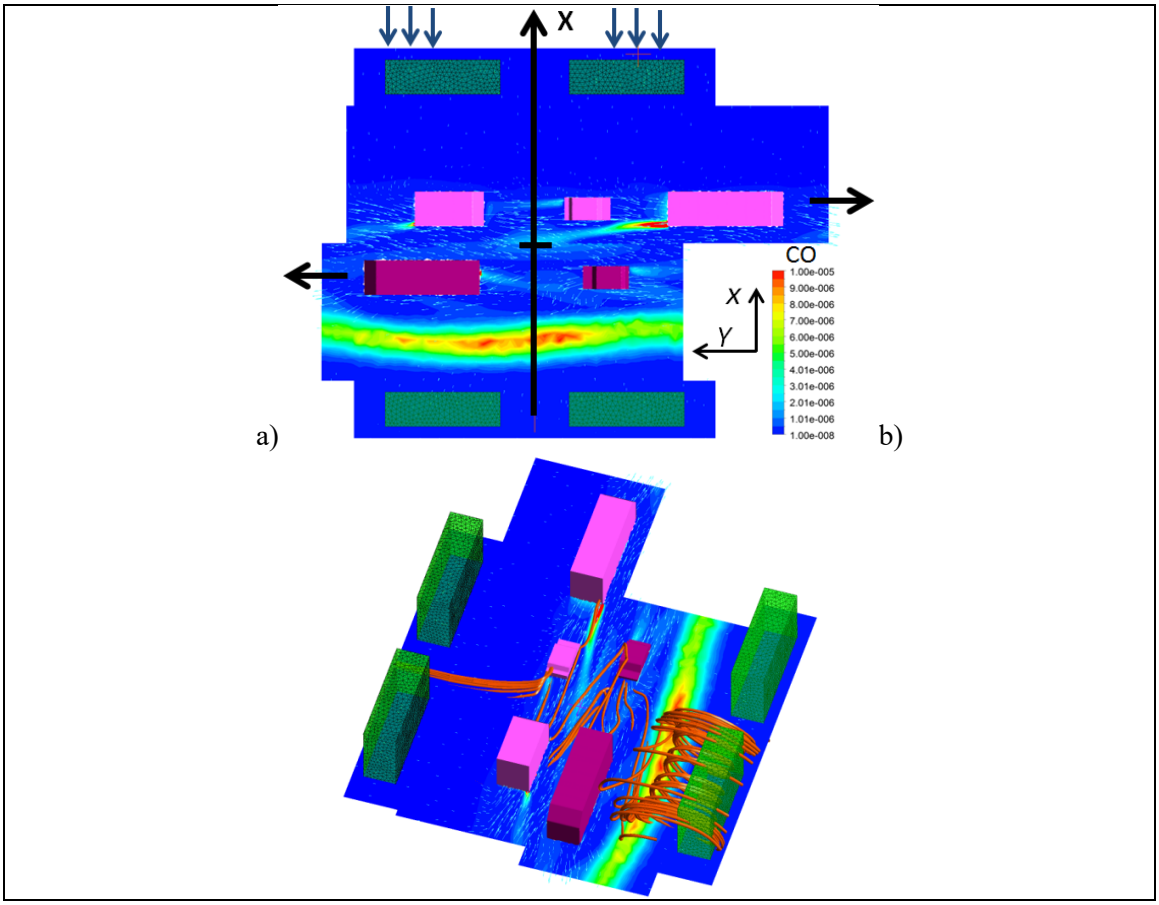

Fig. 3. View of a fragment of a highway: a) and b) show CO mass fraction and streamlines

The concentration scale of the mass fraction of CO emitted by automobiles is divided evenly in the range 0 - 1E-05. Field visualization is presented on a plane 0.5m above the roadway.

In fig. 3b, this same configuration is accompanied by a visualization of airflow lines released from the OX line. The streamlines interact with the traffic flow and overcome the plantings on top. The appearance of the region of maximum values of CO concentration on the side of the road between the lower lane and green spaces is associated with low dynamic wind pressure from the upper side of the road and appears due to the peculiarities of CO drift to the side of the road.

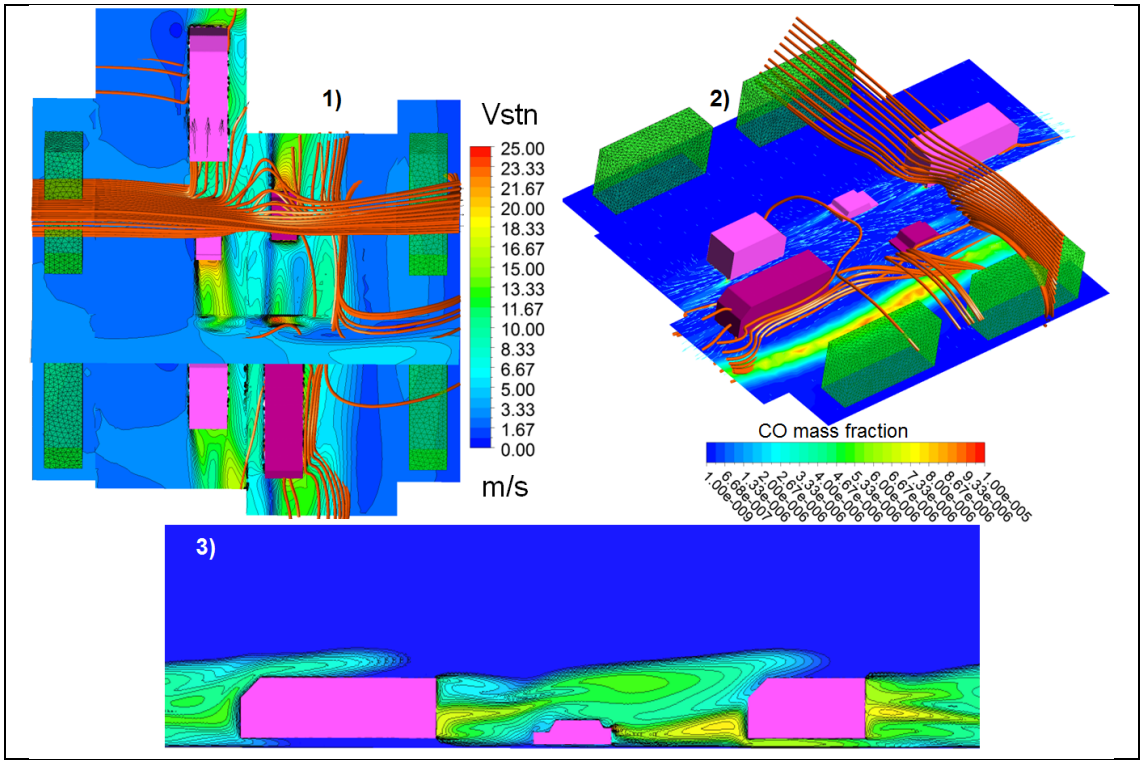

Fig. 4. Flow pattern in representative planes

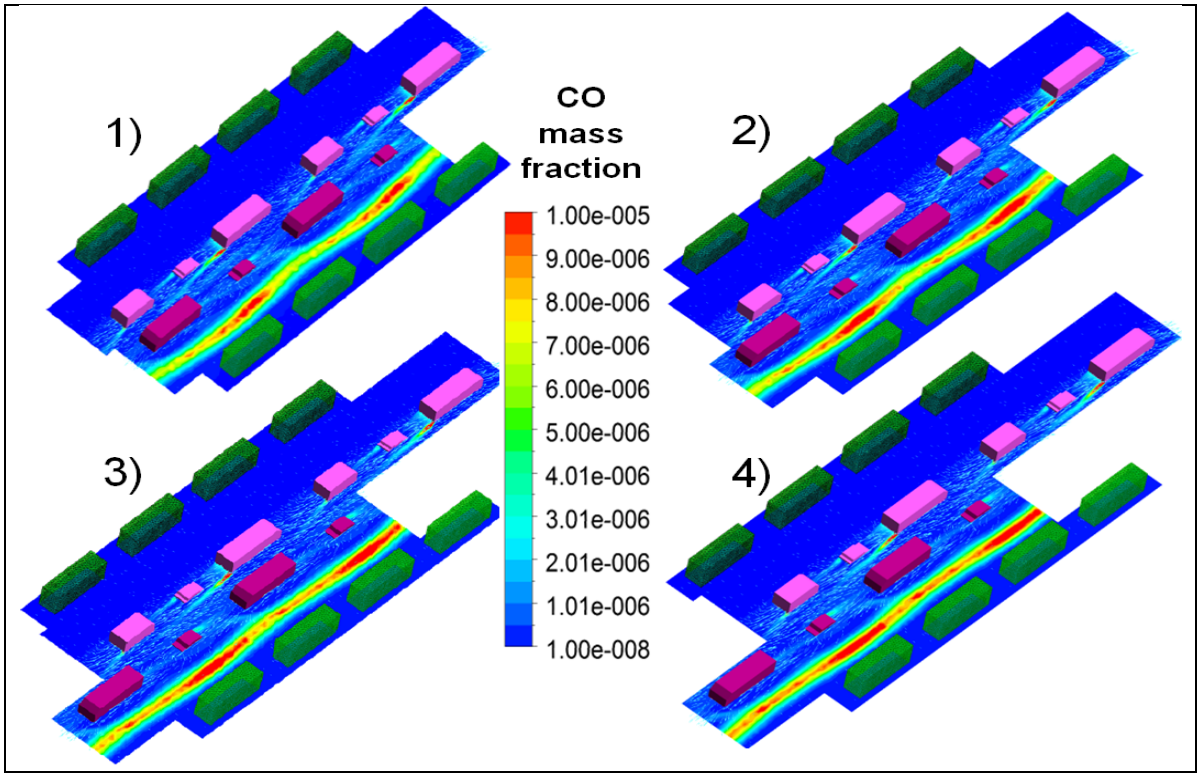

Fig. 5. Four successive points in time during the mutual movement of two transport streams

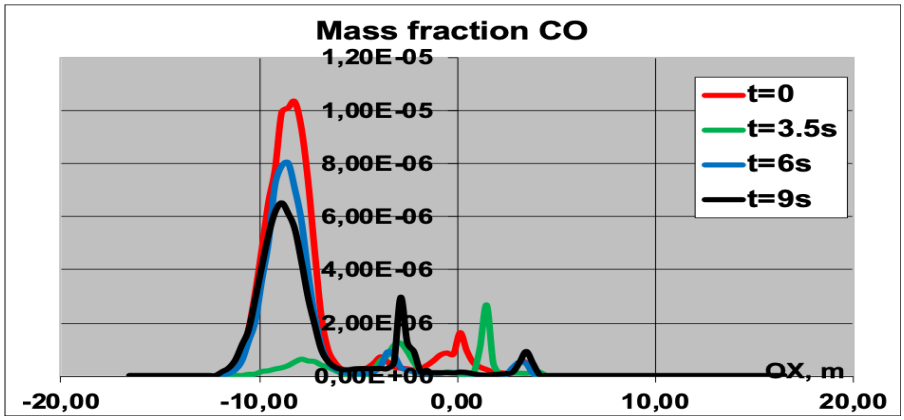

Fig. 6. CO mass fraction distribution along the transversal direction at various time points

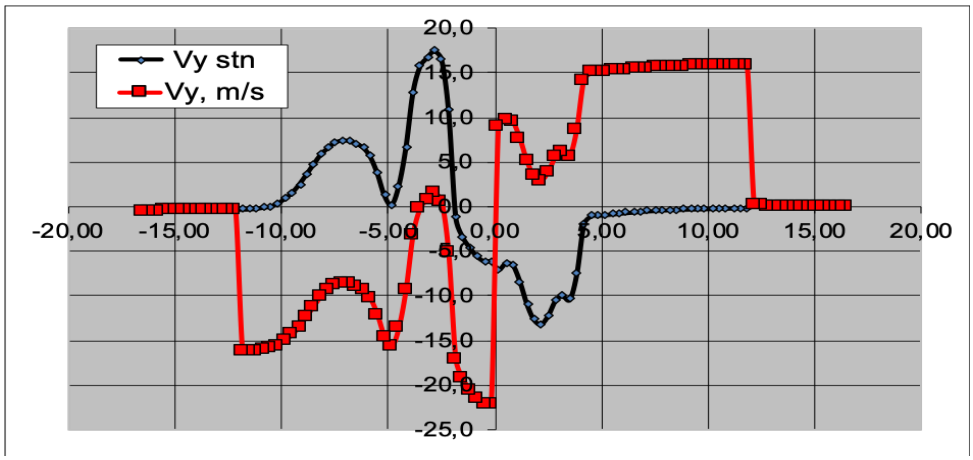

Fig. 7. Longitudinal velocity distribution in absolute ($V_y$stn) and relative (V_y) coordinate systems along the transversal direction of the highway

Fig. 4 presents a depiction of the airflow lines for the variant in Fig. 3, issued uniformly from the vertical windward line. The absolute velocity fields on a surface located 0.6 m above the road surface are also shown. The figures show two views of one event: from above (1) and from the leeward direction (2). Moving motorcades violate the initially uniform structure of streamlines, and the transfer of air mass through the highway is carried out mainly over the top of transport streams. Figure 4 (3) shows the mass fraction of CO in the XOZ plane, which demonstrates the spread of CO pollution.

The series of figures 5 (1-4), which are developed from the motion pattern in Fig. 3, shows four successive points in time during the mutual movement of two transport streams.

The graph in Fig. 6 shows the distribution of the mass fraction of CO in the air along the absolute OX axis. Peaks of CO concentration are unsteady, and correspond to the intersection of the OX axis traces of the CO accumulation region on the side of the road and car exhausts.

The graphs in Fig. 7 represent the distributions of the longitudinal component of air velocity along the OX axis in absolute motion (in blue, from the point of view of the observer on the side of the road) and in relative motion (in red, from the point of view of observers moving in interacting motorcades). This explains the gaps in the velocity distributions in relative motion. According to the diagram (Fig. 4), the direction of the wind is set against the OX axis, and CO concentration is not recorded in the space between the stands and the motorcade on the windward side; it appears when crossing the trace of the exhaust of the truck, and then when crossing the trace from the car, finally reaching its maximum in the space before plantations.

4. CONCLUSION

The proposed model represents the aerodynamic interaction of vehicles in motion along a road section in a tunnel, permitting an arbitrary number of vehicles in each interacting sub-region, and an arbitrary, periodically repeating configuration of vegetation on the sides of the road. This model can be used to predict the distribution of exhaust components in the roadside space as well as the parameters of the interaction forces of bodies. The algorithm of interaction of transport columns is borrowed from the experience of the author, according to the calculations of the flow in mutually moving turbomachine grids. To study the dynamics of a single car, it is sufficient to consider a large-length region containing one car, and use the derivatives of gas-dynamic parameters to be equal to zero at the input/output boundaries.

The flow of atmospheric air and impurities is modeled numerically based on the non-stationary Navier–Stokes equations averaged by Reynolds using the author's *MTFS*® software. Detailing the flow structure allows for an arbitrary length of periodicity, taking into account crosswind. The examples demonstrate some results of the aerodynamic interaction of two oncoming columns of vehicles.

The model can be used to predict the distribution of exhaust components in a roadside space of rather arbitrary configuration, with arbitrary meteorological parameters of the atmosphere. It is possible to generalize this approach for the part of a constant curvature road.

ACKNOWLEDGEMENT

This work was partially funded by the Ministry of Education and Science of Ukraine.

References

1. Larrabee, E. Small Scale Research in Automobile Aerodynamics. *SAE Technical Paper* 660384. 1966. DOI: 10.4271/660384.
2. Goetz, H. The Influence of Wind Tunnel Tests on Body Design, Ventilation, and Surface Deposits of Sedans and Sport Cars. *SAE Technical Paper* 710212. 1971. DOI: 10.4271/710212.
3. Goetz, H. Bus Design Features and their Aerodynamic Effects. Impact of Aerodynamics on Vehicle Design. In: *IAVD Conference, London 1982. Proceedings*. 1983. ISBN 0-907776-01-9.
4. Howell, J. *The Influence of the Proximity of a Large Vehicle on the Aerodynamic Characteristics of a Typical Car. Advances in Road Vehicle Aerodynamics – BHRA.* 1973.
5. Heffley, R. Aerodynamics of Passenger Vehicles in Close Proximity to Trucks and Buses. *SAE Technical Paper* 730235. 1973. DOI: 10.4271/730235.
6. Brown, G. & Seeman, G. An Experimental Investigation of the Unsteady Aerodynamics of Passing Highway Vehicles. *DOT Report DOT-HS-102-1-147*. 1972. See also. Brown, G. Aerodynamic Disturbances Encountered in Highway Passing Situations. *SAE Technical Paper* 730234. 1973. DOI: 10.4271/730234.
7. Telionis, D. & Fahrner, C. & Jones, G. An Experimental Study of Highway Aerodynamic Interferences. *Journal of Wind Engineering and Industrial Aerodynamics*. 1984. Vol. 17. P. 267-293.
8. Emmelmann, H.J. Technologien fur Sicherheit im Strassenverkerh, Einfluss der Luftkrafte auf Fahrdynamik. *Unfallträchtige Fahrsituationen*. P. 308-311. TUV Rheinland GmbH, Koln, 1986.
9. Hucho, W.-H. *Aerodynamics of Road Vehicles*. 4th edition. ISBN 0-7680-0029-7. 1998.
10. Yamamoto, S. & Yanagimoto, K. & Fukuda, H. & China, H. & Nakagawa, K. Aerodynamic Influence of a Passing Vehicle on the Stability of Other Vehicles. *JSAE Review.* 1997. Vol. 18. P. 39-44.
11. Széchényi, E. *The Overtaking Process of Vehicles. Progress in Vehicle Aerodynamics III – Unsteady Flow Effects*. 2004. FKFS Stuttgart.

12. Gilliéron, P. & Noger, C. Contribution to the Analysis of Transient Aerodynamic Effects Acting on Vehicles. *SAE Technical Paper* 2004-01-1311. 2004. DOI: 10.4271/2004-01-1311.
13. Noger, C. & Regardin, C. & Széchényi, E. Investigation of the Transient Aerodynamic Phenomena Associated with Passing Manoeuvres. *Journal of Fluids and Structures.* 2005. Vol. 21. P. 231-241.
14. Schrefl, M. & Mayer, J. & Tropea, C. On the Set-Up of a Surface Pressure Measurement System for On-Road Tests and Preliminary Results Concerning Highway Passing Manoeuvres. In: *6th MIRA International Conference on Vehicle Aerodynamics.* 2006.
15. van Grevenynghe, E. & Noger, C. On the Simulation of Overtaking Manoeuvres in a Full Scale Automotive Wind Tunnel. In: *8th MIRA International Conference on Vehicle Aerodynamics.* 2010.
16. Mayer, J. & Schrefl, M. & Demuth, R. On Various Aspects of the Unsteady Aerodynamic Effects on Cars Under Crosswind Conditions. *SAE Technical Paper* 2007-01-1548. 2007. DOI: 10.4271/2007-01-1548.
17. Howell, J. & Garry, K. & Holt, J. The Aerodynamics of a Small Car Overtaking a Truck. *SAE Int. J. Passeng. Cars - Mech. Syst.* 2014. Vol. 7(2). P. 626-638. DOI: 10.4271/2014-01-0604.
18. Солодов, В. & Філіпов, В. & Жданюк, В. & Кіяшко, І. Математичне моделювання забруднення атмосферного повітря придорожнього простору. *Автошляховик України*. 2009. No 3. P. 42-47. [In Ukrainian: Solodov, V. & Filippov, V. & Zhdaniuk, V. & Kiyasko, I. Mathematical modeling of air pollution of the roadside. *Avtodorozhnik of Ukraine*].
19. Blazek, J. *Computational Fluid Dynamics: Principles and Applications*. Elsevier. 2001. 435 p.
20. *Flow and transport with complex Obstructions. Applications to Cities. Vegetative Canopies and Industry.* Editors Ye. Gayev, Julian Hunt. Springer Publ. 2007. 414 p.
21. Варгафтик, В.Б. *Справочник теплофизических свойств газов и жидкостей.* Москва: Наука. 1972. 720 p. [In Russian: Vargaftik, V.B. *Handbook of thermophysical properties of gases and liquids*. Moscow: Nauka].
22. Солодов, В.Г. & Стародубцев, Ю.В. *Научно-прикладной программный комплекс MTFS® для расчета трехмерных вязких турбулентных течений жидкостей и газов в областях произвольной формы.* Сертификат гос. регистр. авт. прав, УГААСП. No. 5921. 07.16.2002 [In Russian: Solodov, V. & Starodubtsev, Yu. *The Scientific Application Software MTFS® for Calculation of 3D Viscous Turbulent Liquid and Gas Flows in Arbitrary Shape Domains*, Certificate of State Registration, Ukrainian State Agency of Copyrights and Related Rights].
23. Solodov, V.G. & Gnesin, V.I. Nonstationary 3D Numerical Model of Last Turbine Stage – Exhaust Hood Aerodynamical Interaction. *VDI BERICHTE.* 1995. No. 1185. P. 359-373.
24. Говорущенко, Н.Я. & Филиппов, В.В. & Величко, Г.В. Проблемы и методы оценки экологического и энергетического качества автомобильных дорог. *Автоматизированные технологии CREDO*. Минск. 2000. No. 9. P. 45-51. [In Russian: Govorushenko, N.Ya. &, Filippov, V.V. & Velichko, G.V. Problems and Methods for Assessing the Environmental and Energy Quality of Highways. *CREDO automated technologies*. Minsk. 2000. No 9].

Received 10.03.2019; accepted in revised form 10.06.2020